# Formyl Peptide Receptor 2 Plays a Deleterious Role During Influenza A Virus Infections

Sergey Tcherniuk, Nicolas Cenac, Marjorie Comte, Julie Frouard, Elisabeth Errazuriz-Cerda, Angel Galabov, Pierre-Emmanuel Morange, Nathalie Vergnolle, Mustapha Si-Tahar, Marie-Christine Alessi, et al.

**Major Article**

# Formyl peptide receptor 2 plays a deleterious role during influenza A virus infections

Sergey Tcherniuk[1], Nicolas Cenac[2], Marjorie Comte[3], Julie Frouard[3], Elisabeth Errazuriz-Cerda[4], Angel Galabov[5], Pierre-Emmanuel Morange[1], Nathalie Vergnolle[2], Mustapha Si-Tahar[6], Marie-Christine Alessi[1] and Béatrice Riteau[1]

[1]Institut National de la Santé et de la Recherche Médicale (Inserm), UMR_S 1062, 13005 Marseille, France Inra, UMR_INRA 1260, 13005 Marseille, France Aix Marseille Université, 13005 Marseille, France. [2] IRSD, Université de Toulouse, INSERM, INRA, INP-ENVT, Université de Toulouse 3 Paul Sabatier, Toulouse, France. [3]EA4610, Lyon, France; [4]Centre Commun d'Imagerie Quantitative Lyon Est (CIQLE), SFR Santé Lyon-Est, University of Lyon, France. [5]The Stephan Angeloff Institute of Microbiology, Bulgarian Academy of Sciences, Sofia, Bulgaria. [6]INSERM U1100 Université François Rabelais, Tours, France.

Running Title: Formyl peptide Receptor 2 and influenza

**Words text: 2972**

**Words abstract: 296**

**FOOTNOTES**

**Conflict of interest:** The authors declare no conflict of interest.

**Funding statements:** Lipidomic analyses were performed on the Toulouse INSERM Metatoul-Lipidomique Core Facility-MetaboHub ANR-11-INBS-010. This work was also supported by the Agence Nationale de la Recherche (ANR-13-BSV3-0011 to BR).

**Meeting:** This work was never presented in a meeting

**Corresponding author:** Beatrice Riteau: beatrice.riteau@laposte.net

**ABSTRACT**

Background: Pathogenesis of influenza A virus (IAV) infections is a multifactorial process including the replication capacity of the virus and a harmful inflammatory response to infection. Formyl Peptide Receptor 2 (FPR2) emerges as a central receptor in inflammatory processes controlling resolution of acute inflammation. Its role in virus pathogenesis has not been investigated yet.

Methods: We used pharmacologic approaches to investigate the role of FPR2 during influenza A virus infection *in vitro* and *in vivo*.

Results: *In vitro*, FPR2 expressed on A549 cells was activated by IAV which harbor its ligand Annexin-A1 in their envelope. FPR2 activation by IAV promoted viral replication through an extracellular-regulated kinase (ERK)-dependent pathway. *In vivo*, activating FPR2 by administering the agonist WKYMVm-$NH_2$ decreased survival and increased viral replication and inflammation after IAV infection. This effect was abolished by treating the mice with U0126, a specific ERK pathway inhibitor, showing that the deleterious role of FPR2 also occurs through an ERK-dependent pathway, *in vivo*. In contrast, administration of the FPR2 antagonist WRW4 protected mice from lethal IAV infections.

Conclusion: These data show that viral replication and IAV pathogenesis depend on FPR2 signaling and suggest that FPR2 may be a promising novel strategy to treat influenza.

**Key words: Influenza virus, Flu, Host-immune response, Formyl Peptide receptor 2**

## INTRODUCTION

Influenza is an acute respiratory disease responsible for seasonal epidemics and sporadic pandemic outbreaks, leading to significant mortalities in humans [1, 2]. The most severe complication is acute pneumonia, which develops rapidly and may result in respiratory failure and death. Influenza A virus (IAV) pathogenesis is a multifactorial process, involving increased viral replication competence and a harmful inflammatory response. Lipid mediators lipoxins, protectins and resolvins that play a key and active role in the resolution of acute inflammation have received a particular interest in infectious disease lately [3, 4]. Surprisingly, the lipid mediator protectin D1 does not affect inflammatory processes during influenza but inhibits IAV replication and protects mice from severe infection [5]. To date, the contribution of inflammatory pro-resolving receptors that mediate the lipid signaling cascade of lipoxins and protectins mediators to the pathogenesis of IAV infections remains to be determined. Deciphering their role is of crucial importance as these receptors has multiple ligands mediating different functions and these receptors can be used as a novel strategy to fight against severe influenza.

One receptor of interest is the Formyl Peptide Receptor 2 (FPR2/FPRL1/AXL). FPR2 belongs to the seven transmembrane domain of G protein-coupled receptors. FPR2 initiates an active resolution of acute inflammation by binding anti-inflammatory lipid mediators or cellular proteins such as the most prominent lipoxin A4 (LXA4) or the glucocorticoid-modulated protein Annexin-A1 (ANXA1). Although the involvement of FPR2/LXA4 in the resolution of inflammatory responses is now well-recognized both *in vitro* and *in vivo* [6-8], a distinct function of FPR2 includes the detection of bacterial formyl peptides and induction of pro-inflammatory responses [9-11]. Due to the nature of this ligand, FPR2 has also been attributed

77 the label of “pattern recognition receptor”. Thus, FPR2 is emerging as a central checkpoint
78 receptor in inflammatory processes, whose function will most likely depend on accessible
79 ligands and the time course of infection. Studies on the involvement of FPR2 in viral
80 pathogenesis have not been documented so far.
81
82 FPR2 could contribute to the pathogenesis of IAV infections by promoting virus replication
83 and /or a harmful inflammatory response. At present it is unknown whether one or both of
84 these two mechanisms of FPR2 contribute to the pathogenesis of IAV infections. Our findings
85 show that FPR2 plays an important role in modulating lung inflammation and IAV
86 replication, mainly through activation of the ERK pathway. In addition, these results suggest
87 that FPR2 may be explored as a novel target to treat IAV infections.
88
89

## METHODS

### Ethics statement

Experiments were performed according to recommendations of the "National Commission of Animal Experiment (CNEA)" and the "National Committee on the Ethic Reflexion of Animal Experiments (CNREEA)". The protocol was approved by the committee of animal experiments of the Faculty of Marseille la Timone (Permit number: G130555). All animal experiments were also carried out under the authority of license issued by "la direction des services Vétérinaires" (accreditation number 693881479).

### Viruses and reagents

The following reagents were used: IAV A/PR/8/34 (H1N1), A/WSN/33 (H1N1) and A/Udorn/72 (H3N2) IAV, Protease-Activated-receptor 4 agonist AYPGKF-NH2 (Bachem, Bubendorf Switzerland), antagonist of FPR2 WRW4 and agonist of FPR2 WKYMVm-NH2 (R&D Systems, Lille, France), MEK inhibitor U0126 (Promega, Charbonnières, France), siRNA targeting ANXA1, monoclonal anti-ANXA1, polyclonal anti-A5, monoclonal anti-M2 and monoclonal anti-HA (Santa Cruz Biotechnology, Heidelberg, Germany), cholera toxin B subunit and monoclonal anti-tubulin (Sigma Aldrich, Lyon, France), polyclonal anti-ERK and anti-p-ERK (Cell Signalling, Saint Quentin, France), ELISA kits for mouse IL-6 (R&D Systems) and IFN-β (Invitrogen, Cery Pontoise, France).

### Cell culture

The human alveolar A549 and the Madin-Darby canine kidney (MDCK) cell lines were obtained from the American Type Culture Collection (ATCC). MDCK cells were maintained in EMEM (Lonza, Levallois Perret, France) supplemented with 10% Fetal Bovine Serum

(Lonza, France), 2 mM L-glutamine, and penicillin-streptomycin (PS). A549 cells were grown in DMEM (Lonza, France) supplemented with 10% FBS, 2 mM L-glutamine and PS.

**Virus production, titration, purification and immunogold analysis**

Viruses were produced and titrated as previously described [12]. Purified virus particles were obtained from MDCK cells supernatants as done previsouly [13]. Immunogold labeling of ANXA1 and HA was performed on gradient-purified virus particles as previously described [12].

**Flow cytometry, ELISA and western blot analysis**

A549 or MDCK cells were infected or not with A/PR/8/34, A/Udorn/72 or A/WSN/33 (MOI of 1) for 24 hours, and the expression of FPR2 was assessed using flow-cytometry analysis as previously described [14, 15]. ELISA was performed according to the manufacturers' instructions. For western blot analysis, purified virions or cells were lysed and proteins were analyzed, as previsouly described [16].

**ERK activation experiments**

Before lysis for western blot analysis, A549 cells were stimulated with the indicated concentration of FPR2 agonist WKYMVm-NH2 for 5 minutes at 37°C. Regarding the specificity of the WRW4 antagonist (10 µM), cells were first pretreated for 20 minutes at 37°C with FPR2 antagonist WRW4 and stimulated with either 1 µM FPR2 agonist WKYMVm-NH2 or 200 µM PAR4 agonist AYPGKF for 5 minutes at 37°C. For the kinetic of virus-induced ERK phosphorylation, A549 cells were stimulated or not with purified A/WSN/33 virus (MOI 10) for the indicated time point before cell lysis. The effect of FPR2 blockade was assessed as followed: A549 cells were pre-incubated with the indicated

concentration of FPR2 antagonist WRW4 for 20 minutes at 37°C. Cells were then stimulated or not with purified A/WSN/33 or A/Udorn/72 viruses (MOI 10) for 5 minutes in the presence of 60 µM U0126 or vehicle. Stimulation of A549 cells with WT or A1-KD viruses (MOI of 1) was performed for 5 minutes at 37°C in the presence of 60 µM U0126 or vehicle.

**Viral replication experiments**

A549 cells were infected with IAV A/WSN/33 (MOI 1) and stimulated with the indicated concentration of FPR2 agonist, WKYMVm. For FPR2 blockade experiments, A549 cells were first pre-incubated for 20 minutes with 10 µM otherwise indicated of FPR2 antagonist WRW4 for 20 minutes at 37°C before infection. In some experiments, assays were performed in presence of 60 µM U0126 or vehicle. Regarding experiments with IAV harboring KD ANXA1, cells were infected with WT or ANXA1 KO virus at a MOI of 1 in presence of U0126 (60 µM) or vehicle. In all conditions, virus titers were evaluated by plaque assay in the supernatant 16 hours post-inoculation, otherwise indicated. Cell viability in presence of agonist or antagonist of FPR2 was assessed by trypan blue staining 24 hours post-treatment.

**siRNA experiments**

Specific siRNA targeting ANXA1 was used to knock-down protein expression, in A549 cells. Non-targeted siRNA was used as a control, as previously described [12]. Western blot analysis was performed to control the transfection efficiency, 48 hours post-transfection. At this step, control siRNA or targeting ANXA1 siRNA transfected cells were infected with IAV (A/WSN/33 or A/Udorn/72, MOI 1) and supernatants containing the virus particles were harvested 24 hours post-infection and used in experiments. Reduced expression of packaged ANXA1 in the virions released in the supernatant of ANXA1-specific siRNA-treated cells (referred to as A1-KD virus) compared to control viruses (referred to as WT virus) was

confirmed by loading 20µl of the corresponding supernatants on a gel followed by western blot analysis.

**Mouse infection and treatment**

C57BL/6 mice were anesthetized with Ketamine/Xylazine (43/5 mg/kg) and inoculated intranasally with 20 µl of a solution containing A/PR/8/34 virus. Inoculation was made with 500 PFU and 5000 PFU of A/PR/8/34 virus regarding stimulation experiments with the agonist and antagonist of FPR2, respectively. 8 mg/kg FPR2 agonists, FPR2 antagonist or U0126 were administered intraperitoneally. Mice were treated either at days 0, 2 and 4 post-infection or at days 2 and 4 post-infection. For assessing virus replication, broncho-alveolar lavages (BAL) were harvested from sacrificed mice and infectious virus titers were determined by plaque assay, as previously described [12].

**Statistical analysis**

The Mann–Whitney test was used for statistical analysis, regarding viral replication and cytokine production. Kaplan-Meir method was used to calculate the survival fractions in *in vivo* experiments. Two survival curves were compared by the log-rank test (Mantel-Cox test). Results were considered statistically significant at $p < 0.05$ (*).

## RESULTS

### Formyl Peptide Receptor 2 promotes IAV replication

Flow cytometry analysis showed increased FPR2 cell surface expression after infection of the cells with A/Udorn/72, A/PR/8/34, or A/WSN/33 viruses (Figure 1A, left panel). Viral protein M2 was only detected after virus infection. Despite low expression of FPR2 at the surface of uninfected A549 cells, addition of the FPR2 agonist peptide WKYMVm-NH2 (FPR2-AP) to A549 cells triggered ERK phosphorylation (Figure 1A, right panel). Maximal effect was observed at about 1 µM, while the percentage of cell viability was not affected (Figure 1B, left panel). Because ERK phosphorylation is essential for IAV infectivity [17], A549 cells were infected with IAV and stimulated or not with the FPR2-AP. When exposed to the FPR2-AP, infectious virus titers were significantly increased in a dose-dependent manner in the supernatant of these cells compared to vehicle-treated cells (Figure 1B, right panel). Thus, FPR2 activation promotes viral replication during IAV infections, *in vitro*.

### FPR2 antagonist inhibits viral replication

Treatment of IAV-infected A549 cells with FPR2 antagonist WRW4 reduced viral production in a dose- and time course-dependent manner (Figure 1C). WRW4 inhibited the FPR2-AP-induced ERK activation but not the one mediated by PAR4 agonist peptide (Figure 1D, left panel), suggesting that WRW4 blocks FPR2 signalling specifically. Furthermore, WRW4 had no effect on A549 cell viability (Figure 1D, right panel). Thus, FPR2-signaling inhibition blocks viral production in A549-infected cells.

### FPR2 activation by IAV increases viral replication through the ERK pathway

Binding of purified virions to A549 cells for 5 or 10 minutes induced ERK activation (Figure 2A) that was prevented in a dose-dependent manner when cells were pre-incubated with FPR2 antagonist WRW4 (Figure 2B, Vehicle). Similar results were observed using IAV A/Udorn/72. Thus, IAV-FPR2 recognition activated ERK. Then, A/WSN/33 or A/Udorn/72 virus-infected cells were exposed to the FPR2 antagonist in the presence or absence of the ERK signaling-pathway inhibitor U0126. Control experiments showed that U0126 efficiently blocked ERK phosphorylation mediated by IAV recognition of FPR2 on A549 cells (Figure 2B, U0126). As expected, WRW4 treatment decreased virus production by IAV-infected cells (Figures 2C). U0126 also showed antiviral activity in cell culture against IAV. In the presence of U0126 and WRW4, no additional antiviral effect was observed showing that U0126 treatment abolished the difference in viral replication between untreated and WRW4-treated cells. Thus, FPR2 promotes IAV replication through an ERK-dependent pathway.

**Annexin 1 is incorporated into IAV particles**

The ligand on IAV particles that mediated FPR2 activation upon binding to A549 cells was investigated. Proteins from purified IAV A/PR/8/34, A/Udorn/72, and A/WSN/33 were analyzed by Western blot. Results indicated that all purified virions contained the M2 viral protein and ANXA1 (Figure 3A). ERK was only detectable in uninfected and virus infected lysates. Microscopic immunogold analysis also showed a specific immunogold staining of ANXA1 and viral HA on all IAV particles (Figure 3B). Thus, ANXA1 is incorporated into IAV particles. In addition, lipid rafts act as platforms for IAV budding, leading us to investigate whether ANXA1 was upregulated at the cell surface and concentrates in rafts. Results showed that ANXA1 was increased at the surface of infected cells and was enriched in lipid rafts, the site of virus budding (4A-B). Thus, altogether, these results showed that

upon IAV infections, ANXA1 is translocated to the cell membrane, recruited to lipid rafts allowing its incorporation in IAV particles during the budding process.

**Annexin 1 incorporated into IAV promotes viral replication**

Wild-type (WT) virions or virions for which ANXA1 was knock-down by silencing gene expression (A/WSN/33 and A/Udorn/72 strains) were generated. Western blot analysis confirmed that A549 cells transfected with the siRNA targeting ANXA1, express less ANXA1, but did not affect A5 protein expression, compared to A549 cells transfected with a siRNA control (Figure 5A). Viruses released by these cells were knock-down for ANXA1 levels (A1-KD virus) compared to siRNA control viruses (WT virus) (Figure 5B). Binding of WT virus to A549 cells induced ERK activation (Figure 5C, Vehicle). This activation was strongly impaired after incubation with A1-KD virus. Also, WT virus replicated more efficiently compared to A1-KD virus (Figure D, Vehicle). In the conditions where U0126 efficiently blocked virus-induced ERK activation (Figure 5D, U0126), this difference in virus fitness was abolished. Thus, ANXA1 incorporated in IAV is responsible for ERK activation upon IAV binding to the cells and increases virus replication.

**FPR2 contributes to the pathogenesis of IAV infection**

Mice were infected with IAV A/PR/8/34 and treated or not with FPR2-AP, WKYMVm-NH2. Infected mice treated with the FPR2-AP displayed significant increased mortality rates, compared to control-treated mice (Figure 6A, left panel). FPR2-AP had no effect on uninfected mice (Figure 6A, right panel). At days 3 or 6 after inoculation, lung virus titers and cytokine production were significantly increased after FPR2-AP treatment (Figure 6B-C).

Thus, FPR2-signaling enhanced IAV pathogenesis which correlated with increase viral titers and inflammation in the lungs.

**The effect of FPR2 activation occurs through an ERK dependent pathway**

Infected mice were treated or not with the ERK inhibitor U0126 in presence or absence of FPR2-AP treatment. In contrast to untreated mice, treatment of mice with U0126 abrogated the effect of FPR2-AP on mortality rates after IAV infection (Figure 6D). Thus, the role of FPR2 in IAV pathogenesis occurs through an ERK signaling pathway *in vivo*.

**FPR2 antagonist protects against IAV infection**

Mice treated with FPR2 antagonist WRW4 were more resistant to A/PR/8/34 infection than vehicle-treated mice (Figure 7A). No effect was observed on uninfected mice. Protection mediated by WRW4 correlated with reduced lung virus titers and inhibition of cytokines IL6 and INFβ production (Figure 7B and 7C). Interestingly, when WRW4 was administered from day 2 post inoculation onward, mice were also significantly protected from A/PR/8/34 and A/Hong-Kong/68 virus infections (Figure 7D). Thus, inhibition of FPR2-signaling protect mice from IAV replication in the lungs, inflammation and severe disease development.

## DISCUSSION

The present study showed that FPR2 plays an important role during IAV infections. *In vitro*, stimulation of FPR2 using specific agonists increased viral replication while blocking FPR2 with a specific FPR2 inhibitor did the opposite, indicating that FPR2-signaling plays a pro-viral effect during IAV infections. Consistent with our *in vitro* studies, FPR2-AP promoted virus replication and exacerbated the effects of IAV infection in infected mice. Moreover, FPR2-antagonist-treated mice were protected from IAV infection showing that FPR2 activation contributes to the pathogenesis of IAV infection.

To our knowledge, a role for FPR2 in the pathogenesis of virus infections using *in vivo* models has not been previously described. FPR2 activation did not exacerbate the effects of IAV infection in mice treated with an inhibitor of ERK activation. Thus, ERK is playing a permissive role for the effect of FPR2 activation in IAV infection. Our observation that FPR2 promoted an ERK-dependent proviral effect in lung epithelial cultures and in the lungs of infected mice demonstrate a link between FPR2 signaling, ERK activation and the ability of IAV to replicate. Interestingly, our results showed that FPR2 inhibition induces the late production of protectins in the lungs of infected mice (S2 Fig.), suggesting that FPR2 signaling blocks the production of protectin generation. This observation is of particular interest since protectin attenuates IAV replication though inhibition of virus RNA export [5], a step which requires signalling through the ERK cascade [17]. Thus, it is possible that FPR2 signaling inhibits protectin generation, leading to RNA export and virus replication.

The endogenous activators of FPR2 in the airways are not well characterized. FPR2 expressed by respiratory epithelial cells as well as leucocytes is susceptible to be activated by various ligands of diverse classes and from different sources. The observation that ANXA1 is incorporated into IAV particles and that ANXA1-deficient virions have no effect on FPR2-

signaling suggests that the first ligand that maybe involved at an early stage during IAV infection could be ANXA1 which was incorporated into IAV particles. Interestingly, FPR2-binding to peptides derived from the envelope protein gp41 of human immunodeficiency viruses (HIV) acts as an efficient coreceptor for virus entry [18, 19]. Thus, several strategies seems to be developed by different viruses to activate FPR2 for efficient replication, highlighting an emerging role for FPR2 during viral infections. Possibly, the extent of ANXA1 incorporation into IAV particles in a strain-dependent manner may explain differences in pathogenicity of IAV strains through activation FPR2.

Formylated peptides are the prototypical ligands for FPR2 and to our knowledge, bacterial and mitochondrial proteins are the only source of N-formyl peptides [10, 20]. However, a broad range of non-N formyl and protein ligands have also been identified, including lipid metabolites such as LXA4, in addition to cellular ANXA1. In this context, activation of FPR2 rather elicits anti-inflammatory and pro-resolving reactions in several models of acute inflammation [21]. The fact that ANXA1 was incorporated into IAV suggests that as soon as IAV infects a cell, FPR2 is activated. Thus, it is most likely that IAV developed mechanisms to escape immune surveillance by inhibiting the host immune response through ANXA1/FPR2 before acute inflammation occurs. This dampened early immune response together with an increase virus replication might be responsible for a subsequent harmfull inflammation of the lungs. Indeed, excessive inflammation is a well-known contributor of lung damage during severe influenza, a process that limits respiratory capacity and may account for IAV pathogenesis in humans [1, 22]. Consistently, along with increased viral replication, FPR2 exacerbated lung inflammation during IAV infection, in mice. To our knowledge, the role of FPR2 in the inflammatory process of virus infections has not been previously described. Increase inflammation mediated by FPR2 might also be the consequence of a direct activation of the ERK pathway, a known signaling mediator of

inflammation [23]. FPR2 controls platelet/neutrophil aggregates leading to the rapid generation of circulating LXA4 that subsequently further activates FPR2 [24]. Thus, the involvement of a dysregulated platelet activation, known to promote acute lung injury during influenza cannot also be ruled out in the deleterious role of FPR2 [25, 26].

Altogether our results show that FPR2 is an important receptor involved in IAV pathogenesis, acting both at the level of IAV replication and inflammation. Our results also suggest that inhibitors of FPR2 should be explored as a novel strategy for the treatment of IAV infections.

## FIGURES LEGENDS

**Figure 1: Cell surface expression and function of FPR2 during IAV infections.**

(A, left panel) A549 cells were infected with A/PR/8/34, A/Udorn/72 or A/WSN/33 viruses (MOI of 1). Twenty four hours post-infection, cell surface expression of FPR2 was evaluated by flow cytometry analysis using an anti-FPR2 antibody (open histograms) or an isotype control (closed histograms). The viral protein M2 protein was used as a positive control for viral infection. Results are representative of two independent experiments. (A, right panel) A549 cells were treated with the indicated concentrations of FPR2-AP for 5 minutes at 37°C. Cells were then lysed and ERK phosphorylation was analyzed by western blot using an anti-phospho ERK antibody (p-ERK). Total ERK protein was used as a loading control. (B, left panel) A549 cells were treated with the indicated concentrations of FPR2-AP for 24 hours. Cell viability was then estimated by trypan blue staining. Results show the mean values ± standard deviations from three independent experiments. (B, right panel) A549 cells were infected or not with IAV A/WSN/33 and treated with the indicated concentration of FPR2-AP. Sixteen hours post-infection, infectious virus titers were determined by plaque assay. (C, left panel) A549 cells were pre-treated with the indicated concentrations of FPR2-antagonist, and infected with IAV A/WSN/33 at a MOI of 1. Thirty-six hours post-infection, infectious virus titers were determined by plaque assay. (C, right panel) A549 cells were pre-treated with 10 µM of FPR2-antagonist and infected with A/WSN/33 virus at an MOI of 1. After the indicated time points post-infection, infectious virus titers were determined by plaque assay. (D, left panel) A549 cells were pre-incubated with FPR2-antagonist and treated with 1 µM of FPR2-AP or 200 µM PAR4-AP. ERK activation was then evaluated by western blot analysis. (D, right panel) A549 cells treated with the indicated concentrations of WRW4 FPR2-

antagonist for 24 hours. Cell viability was estimated by trypan blue staining. Results show the mean values ± standard deviations from three independent experiments.

**Figure 2: Influenza virus activates FPR2-induced ERK activation and virus replication**

(A) A549 cells were incubated with purified A/WSN/33 particles (MOI 10). After cell lysis, ERK phosphorylation was analysed by western blot at the indicated time points post-infection. (B) A549 cells were pretreated with the indicated concentration of FPR2-antagonist for 20 minutes and incubated 5 minutes with purified A/WSN/33 or A/Udorn/72 particles (MOI 10) in presence of vehicle or U0126 (60 µM). After cell lysis, ERK activation was analysed by western blot. (C) A549 cells were pre-incubated with FPR2-antagonist (10 µM, 20 minutes) and infected with purified A/WSN/33 or A/Udorn/72 particles (MOI 10) in presence of vehicle or U0126 (60 µM). Thirty-six hours post-infection, infectious virus titers were determined by plaque assay.

**Figure 3: ANXA1 incorporation into IAV particles**

(A) Proteins from purified A/PR/8/34, A/Udorn/72 and A/WSN/33 viruses were analysed by western blot using anti-ANXA1, anti-M2 and anti-ERK antibodies. Aliquots of total proteins from uninfected or A/PR/8/34 virus infected MDCK cells were used as controls. Protein molecular weight was presented in kDa. Results are representative of three independent experiments. (B) IAV A/PR/8/34, A/Udorn/72 and A/WSN/33 viruses were produced in MDCK cells and purified by sucrose gradient ultracentrifugation. Electron microscopic immunogold labeling was performed on the purified virions using anti-ANXA1 and anti-HA antibodies. Bar is 50 nm. Results are representative of two independent experiments.

.

**Figure 4: ANXA1 expression at the cell surface and in the lipid rafts after IAV infection**

(A) Detection of cell surface ANXA1 in A549 (upper panels) or MDCK cells (lower panels) after infection with A/Udorn/72, A/PR/8/34 or A/WSN/33 virus (MOI 1, 24 hours) by flow cytometry using an anti-ANXA1 antibody (open histograms) or an isotype control antibody (closed histograms). The viral protein M2 was used as a positive marker for viral infection. Results are representative of two independent experiments. (B) A549 cells were left uninfected or were infected with A/WSN/33 virus for 16 hours at a MOI of 1.

After cell lysis, the rafts domains were isolated by sucrose gradient ultracentrifugation. Fractions 1-10 were then collected from the top of the tube and proteins within each fractions were characterized by western blot analysis. Blots were probed with cholera-toxin B subunit (GM1) or anti-ERK (ERK), anti-HA (HA0-HA2), anti-M2 and anti–ANXA1 (ANXA1) antibodies. Fractions 3-4 and 9-10 correpond to rafts and soluble fractions, respectively.

**Figure 5: Effect of packaged ANXA1 on virus replication and involvement of the ERK pathway**

(A) A549 cells were transfected with siRNA targeting ANXA1 at the indicated concentration (siRNA) or 80 nM of control siRNA (-). Forty eight hours post-transfection, cells were lysed and proteins from the lysates were analysed by western blot using an anti-ANXA1 or anti-A5 antibodies. (B) A1-KD and WT viruses were harvested from the supernateants of infected A549 cells transfected with siRNA targeting ANXA1 or control siRNA, respectively. After virus lysis, proteins from were characterized by western blot, using anti-ANXA1, anti-M2 and anti–ERK antibodies. Lysates from uninfected or A/PR/8/34 virus infected A549 cells were used as controls. (C) A549 cells were incubated 5 minutes with A1-KD virus or WT virus (MOI 1) in presence of vehicle or U0126 (60 µM). After cell lysis, proteins were analysed by

406 western blot using the anti p-ERK or anti ERK antibodies. (D) A549 cells were infected with
407 WT virus or A1-KD virus (MOI 1, 16 hours) in presence of vehicle or U0126 (60 µM) and
408 infectious virus titers were determined by plaque assay.
409
410 **Figure 6: Effect of FPR2 activation on IAV pathogenicity**
411 (A) Time course of IAV-induced pathogenesis and death in mice in response to FPR2
412 stimulation. Mice were inoculated intranasally with A/PR/8/34 virus (500 PFU, n = 13-
413 15/group) and treated with vehicle or FPR2-AP (8 mg/kg upper panel). Alternatively, mice
414 were left uninfected and treated or not with FPR2-AP (n = 8-12/group, down panel). Results
415 show the average percent survival from 2 experiments. (B) infectious virus titers in the BAL
416 of infected mice treated or not with 8 mg/kg of FPR2-AP. Data are average ± SD from 6
417 animals per group. (C) Levels of IFN-β and IL-6 in the BAL of A/PR/8/34 virus infected
418 mice treated with FPR2-AP WKYMVm-NH2 (8mg/kg) or vehicle (1% DMSO); n= 3-
419 6/group. (D) After treatment with U0126 (8mg/kg) or vehicle (Untreated), mice were
420 inoculated with A/PR/8/34 virus (250 PFU, n = 6/group) and stimulated or not with FPR2-AP
421 (8 mg/kg). Mice were then followed for survival.
422
423 **Figure 7: Antiviral effect of FPR2 antagonist**
424 (A) Survival of A/PR/8/34 virus infected mice (n=7/group, upper panel) or uninfected mice
425 (down panel, n=12/group) after treatment with FPR2 antagonist at days 0, 2 and 4 post-
426 infection (B) Infectious lung virus titers in vehicle or FPR2 antagonist-treated mice. Data
427 represent mean ± s.e.m of 5-6 individual mice per group. (C) IFN-β and IL-6 analysis in the
428 BAL of virus-infected mice (n= 3-5/group) treated with FPR2 antagonist or vehicle. (D) Mice
429 were inoculated with IAV A/PR/8/34 (n=18/group) or A/HK/68 (n=6/group), as indicated.
430 FPR2 treatment was initiated two days post-inoculation.

## REFERENCES


1. Kuiken T, Riteau B, Fouchier RA, Rimmelzwaan GF. Pathogenesis of influenza virus infections: the good, the bad and the ugly. Curr Opin Virol **2012**; 2:276-86.

2. Fukuyama S, Kawaoka Y. The pathogenesis of influenza virus infections: the contributions of virus and host factors. Current opinion in immunology **2011**; 23:481-6.

3. Serhan CN. Pro-resolving lipid mediators are leads for resolution physiology. Nature **2014**; 510:92-101.

4. Russell CD, Schwarze J. The role of pro-resolution lipid mediators in infectious disease. Immunology **2014**; 141:166-73.

5. Morita M, Kuba K, Ichikawa A, et al. The lipid mediator protectin D1 inhibits influenza virus replication and improves severe influenza. Cell **2013**; 153:112-25.

6. Perretti M, Chiang N, La M, et al. Endogenous lipid- and peptide-derived anti-inflammatory pathways generated with glucocorticoid and aspirin treatment activate the lipoxin A4 receptor. Nature medicine **2002**; 8:1296-302.

7. Chiang N, Serhan CN, Dahlen SE, et al. The lipoxin receptor ALX: potent ligand-specific and stereoselective actions in vivo. Pharmacological reviews **2006**; 58:463-87.

8. Perretti M, D'Acquisto F. Annexin A1 and glucocorticoids as effectors of the resolution of inflammation. Nat Rev Immunol **2009**; 9:62-70.

9. De Y, Chen Q, Schmidt AP, et al. LL-37, the neutrophil granule- and epithelial cell-derived cathelicidin, utilizes formyl peptide receptor-like 1 (FPRL1) as a receptor to chemoattract human peripheral blood neutrophils, monocytes, and T cells. J Exp Med **2000**; 192:1069-74.

10. Carp H. Mitochondrial N-formylmethionyl proteins as chemoattractants for neutrophils. J Exp Med **1982**; 155:264-75.

11. Liu M, Chen K, Yoshimura T, et al. Formylpeptide receptors are critical for rapid neutrophil mobilization in host defense against Listeria monocytogenes. Sci Rep **2012**; 2:786.

12. Berri F, Haffar G, Le VB, et al. Annexin V incorporated into influenza virus particles inhibits gamma interferon signaling and promotes viral replication. J Virol **2014**; 88:11215-28.

13. LeBouder F, Morello E, Rimmelzwaan GF, et al. Annexin II incorporated into influenza virus particles supports virus replication by converting plasminogen into plasmin. J Virol **2008**; 82:6820-8.

14. LeBouder F, Khoufache K, Menier C, et al. Immunosuppressive HLA-G molecule is upregulated in alveolar epithelial cells after influenza A virus infection. Hum Immunol **2009**; 70:1016-9.

15. Riteau B, Moreau P, Menier C, et al. Characterization of HLA-G1, -G2, -G3, and -G4 isoforms transfected in a human melanoma cell line. Transplant Proc **2001**; 33:2360-4.

16. Riteau B, Barber DF, Long EO. Vav1 phosphorylation is induced by beta2 integrin engagement on natural killer cells upstream of actin cytoskeleton and lipid raft reorganization. J Exp Med **2003**; 198:469-74.

17. Pleschka S, Wolff T, Ehrhardt C, et al. Influenza virus propagation is impaired by inhibition of the Raf/MEK/ERK signalling cascade. Nature cell biology **2001**; 3:301-5.

18. Shimizu N, Tanaka A, Mori T, et al. A formylpeptide receptor, FPRL1, acts as an efficient coreceptor for primary isolates of human immunodeficiency virus. Retrovirology **2008**; 5:52.

19. Shimizu N, Tanaka A, Oue A, et al. Broad usage spectrum of G protein-coupled receptors as coreceptors by primary isolates of HIV. AIDS **2009**; 23:761-9.

20. Schiffmann E, Showell HV, Corcoran BA, Ward PA, Smith E, Becker EL. The isolation and partial characterization of neutrophil chemotactic factors from Escherichia coli. J Immunol **1975**; 114:1831-7.

21. Oldekamp S, Pscheidl S, Kress E, et al. Lack of formyl peptide receptor 1 and 2 leads to more severe inflammation and higher mortality in mice with of pneumococcal meningitis. Immunology **2014**; 143:447-61.

22. de Jong MD, Simmons CP, Thanh TT, et al. Fatal outcome of human influenza A (H5N1) is associated with high viral load and hypercytokinemia. Nature medicine **2006**; 12:1203-7.

23. Kurosawa M, Numazawa S, Tani Y, Yoshida T. ERK signaling mediates the induction of inflammatory cytokines by bufalin in human monocytic cells. American journal of physiology Cell physiology **2000**; 278:C500-8.

24. Brancaleone V, Gobbetti T, Cenac N, et al. A vasculo-protective circuit centered on lipoxin A4 and aspirin-triggered 15-epi-lipoxin A4 operative in murine microcirculation. Blood **2013**; 122:608-17.

25. Le VB, Schneider JG, Boergeling Y, et al. Platelet activation and aggregation promote lung inflammation and influenza virus pathogenesis. Am J Respir Crit Care Med **2015**; 191:804-19.

26. Sugiyama MG, Gamage A, Zyla R, et al. Influenza Virus Infection Induces Platelet-Endothelial Adhesion Which Contributes to Lung Injury. J Virol **2015**; 90:1812-23.

**Fig 1**

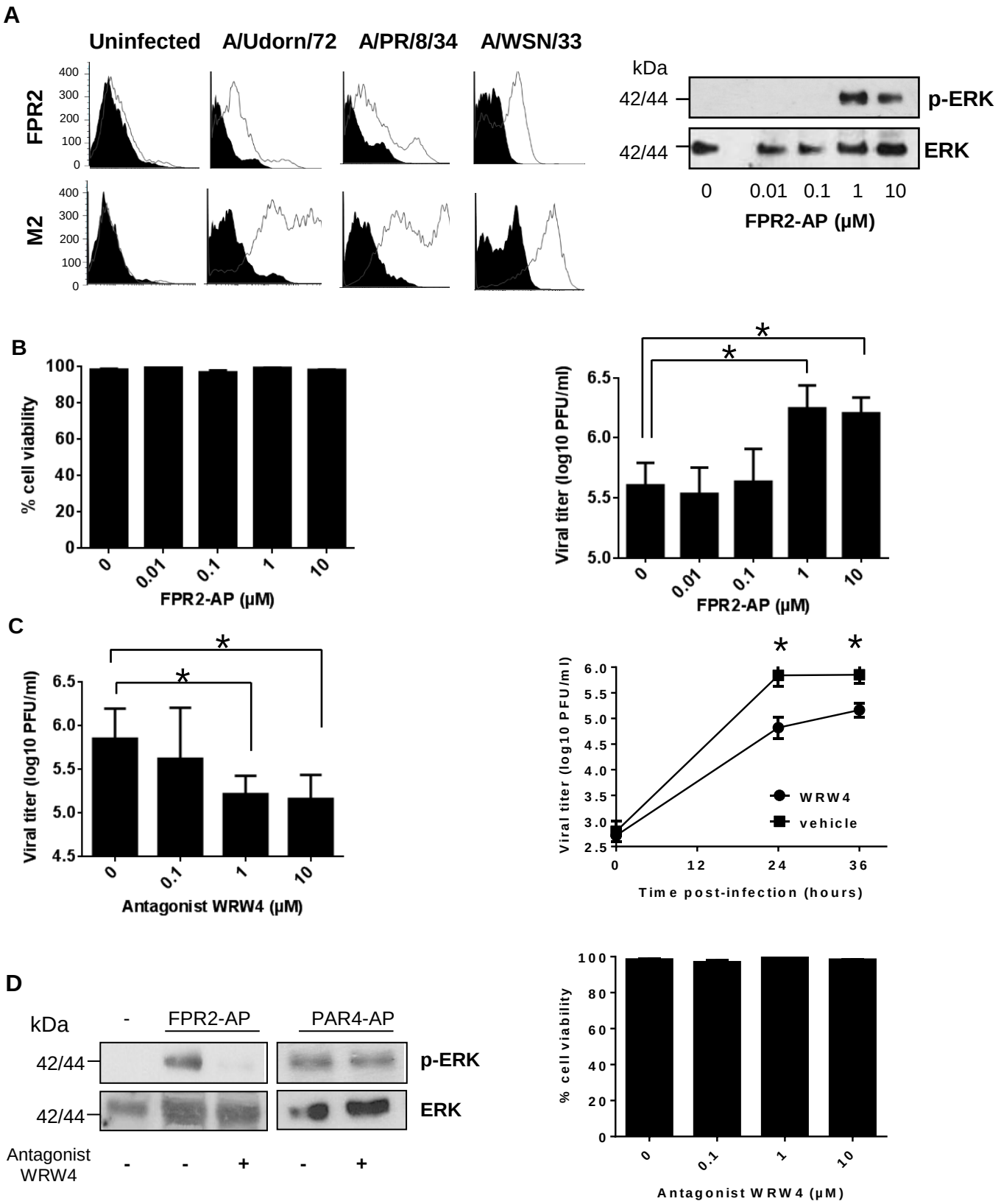
A
Uninfected
A/Udorn/72
A/PR/8/34
A/WSN/33
FPR2
M2
400
300
200
100
0
kDa
42/44
p-ERK
ERK
0
0.01
0.1
1
10
FPR2-AP (μM)
B
% cell viability
100
80
60
40
20
0
FPR2-AP (μM)
Viral titer (log10 PFU/ml)
6.5
6.0
5.5
5.0
C
4.5
Antagonist WRW4 (μM)
WRW4
vehicle
Time post-infection (hours)
0
12
24
36
D
FPR2-AP
PAR4-AP
Antagonist WRW4
-
+

**Fig 2**

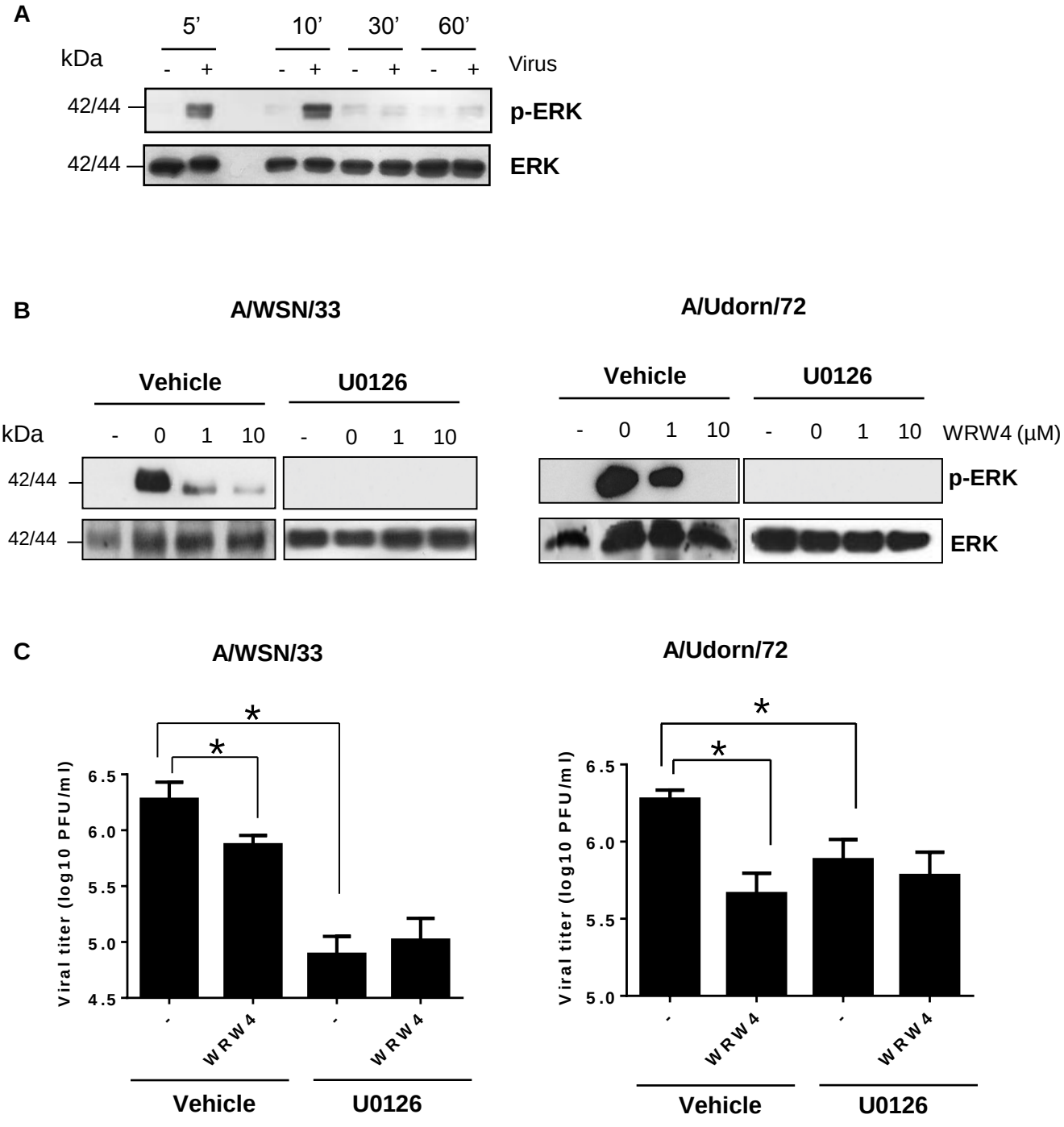
A
5'
10'
30'
60'
kDa
- + - + - + - +
Virus
42/44
p-ERK
42/44
ERK
B
A/WSN/33
A/Udorn/72
Vehicle
U0126
Vehicle
U0126
kDa
- 0 1 10 - 0 1 10
- 0 1 10 - 0 1 10
WRW4 (μM)
42/44
p-ERK
42/44
ERK
C
A/WSN/33
A/Udorn/72
Viral titer (log10 PFU/ml)
6.5
6.0
5.5
5.0
4.5
*
*
WRW4
Vehicle
U0126

**Fig 3**

**A**

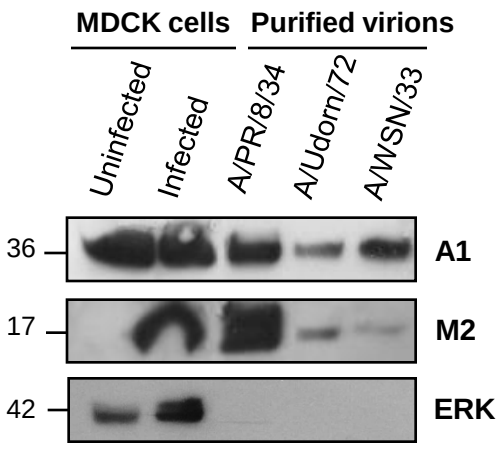
MDCK cells
Purified virions
Uninfected
Infected
A/PR/8/34
A/Udorn/72
A/WSN/33
36
A1
17
M2
42
ERK

**B**

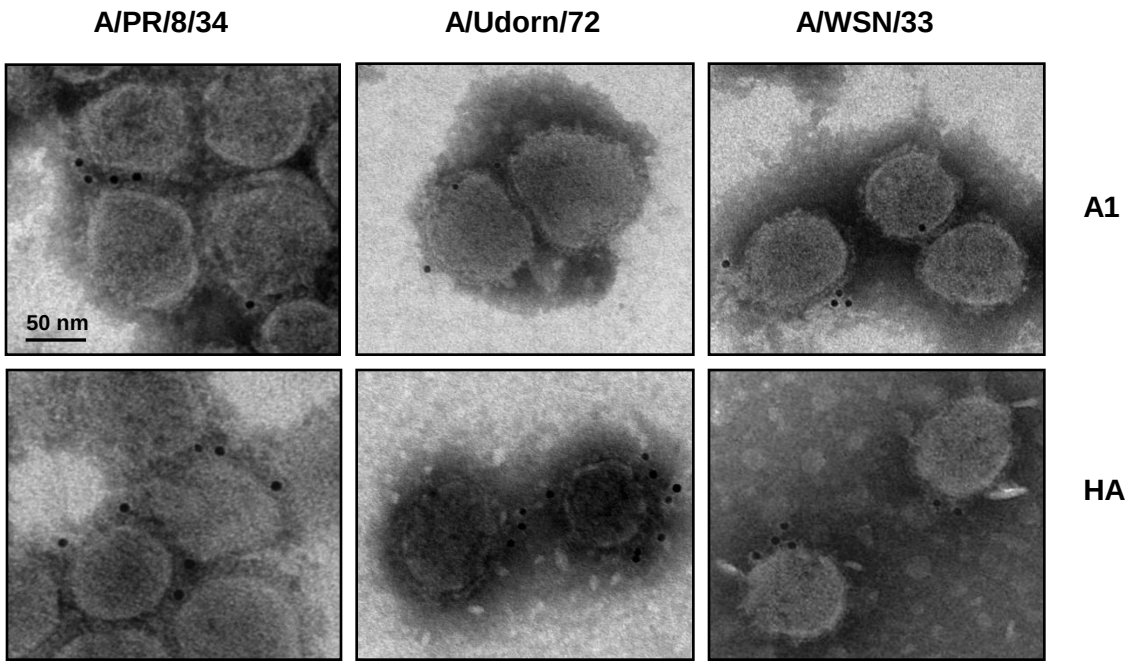
A/PR/8/34
A/Udorn/72
A/WSN/33
50 nm
A1
HA

**Fig 4**

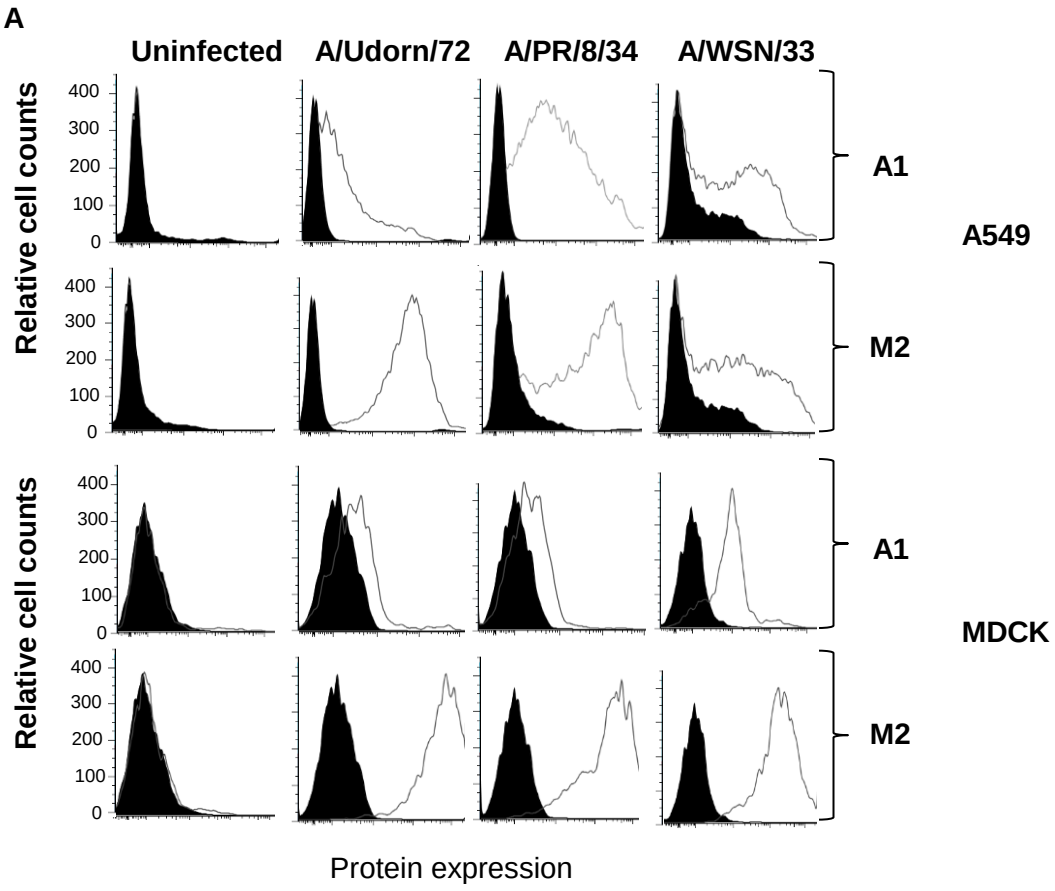
A
Uninfected
A/Udorn/72
A/PR/8/34
A/WSN/33
Relative cell counts
400
300
200
100
0
A1
A549
M2
Relative cell counts
A1
MDCK
M2
Protein expression

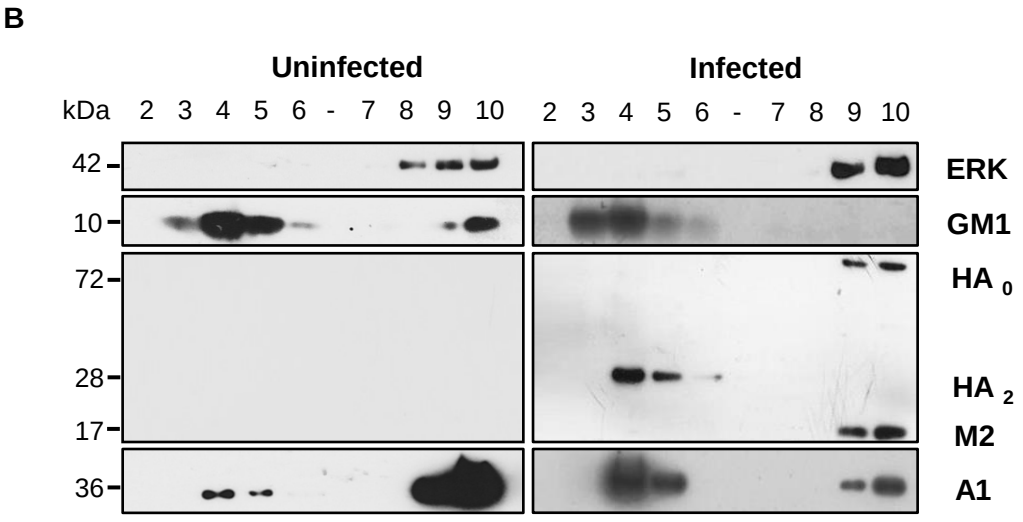
B
Uninfected
Infected
kDa
2 3 4 5 6 - 7 8 9 10
2 3 4 5 6 - 7 8 9 10
42
10
72
28
17
36
ERK
GM1
HA 0
HA 2
M2
A1

**Fig 5**

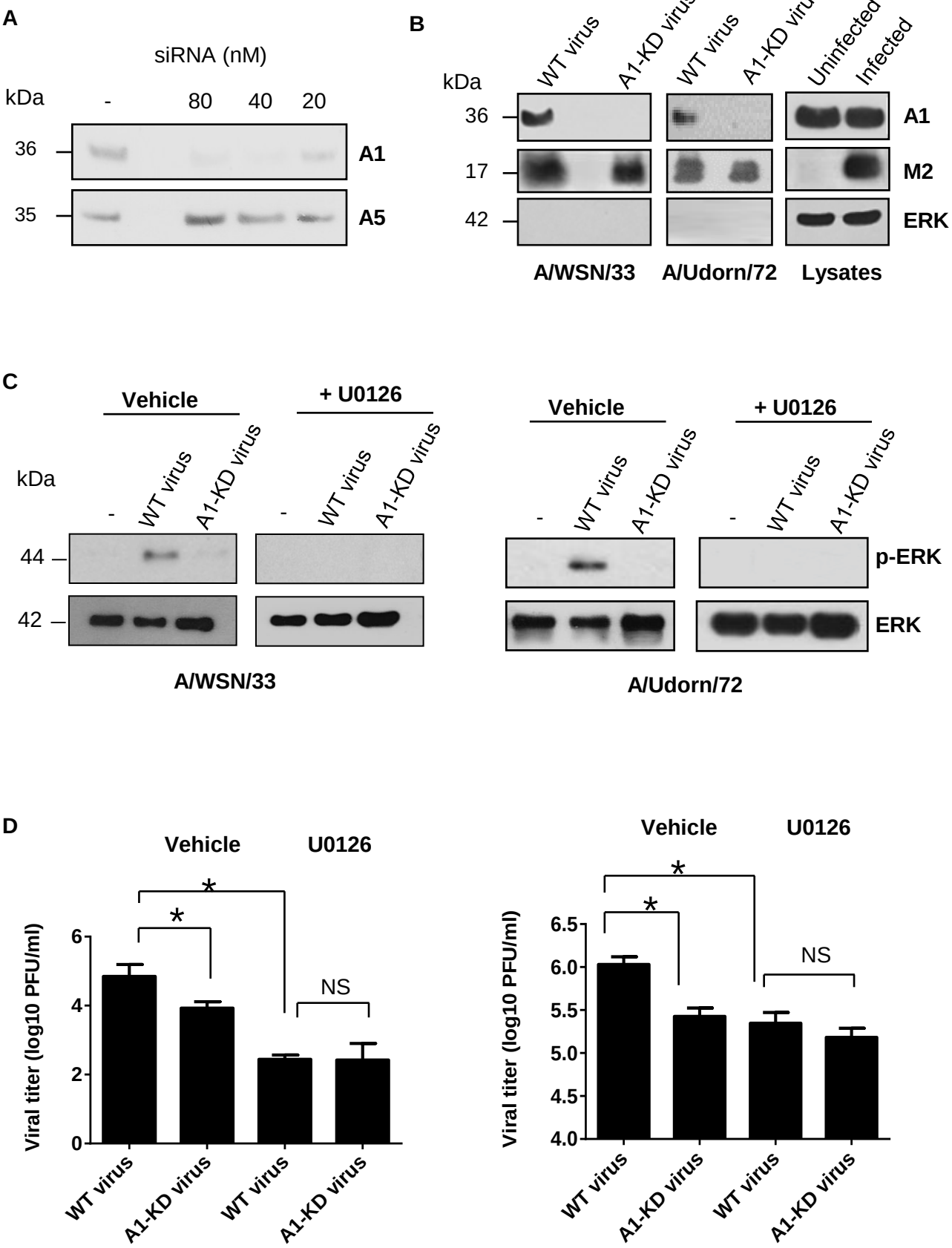
A
siRNA (nM)
kDa
-
80
40
20
36
A1
35
A5
B
kDa
WT virus
A1-KD virus
WT virus
A1-KD virus
Uninfected
Infected
36
17
42
A1
M2
ERK
A/WSN/33
A/Udorn/72
Lysates
C
Vehicle
+ U0126
kDa
WT virus
A1-KD virus
44
42
p-ERK
ERK
A/WSN/33
A/Udorn/72
D
Vehicle
U0126
Viral titer (log10 PFU/ml)
NS
WT virus
A1-KD virus

Fig 6

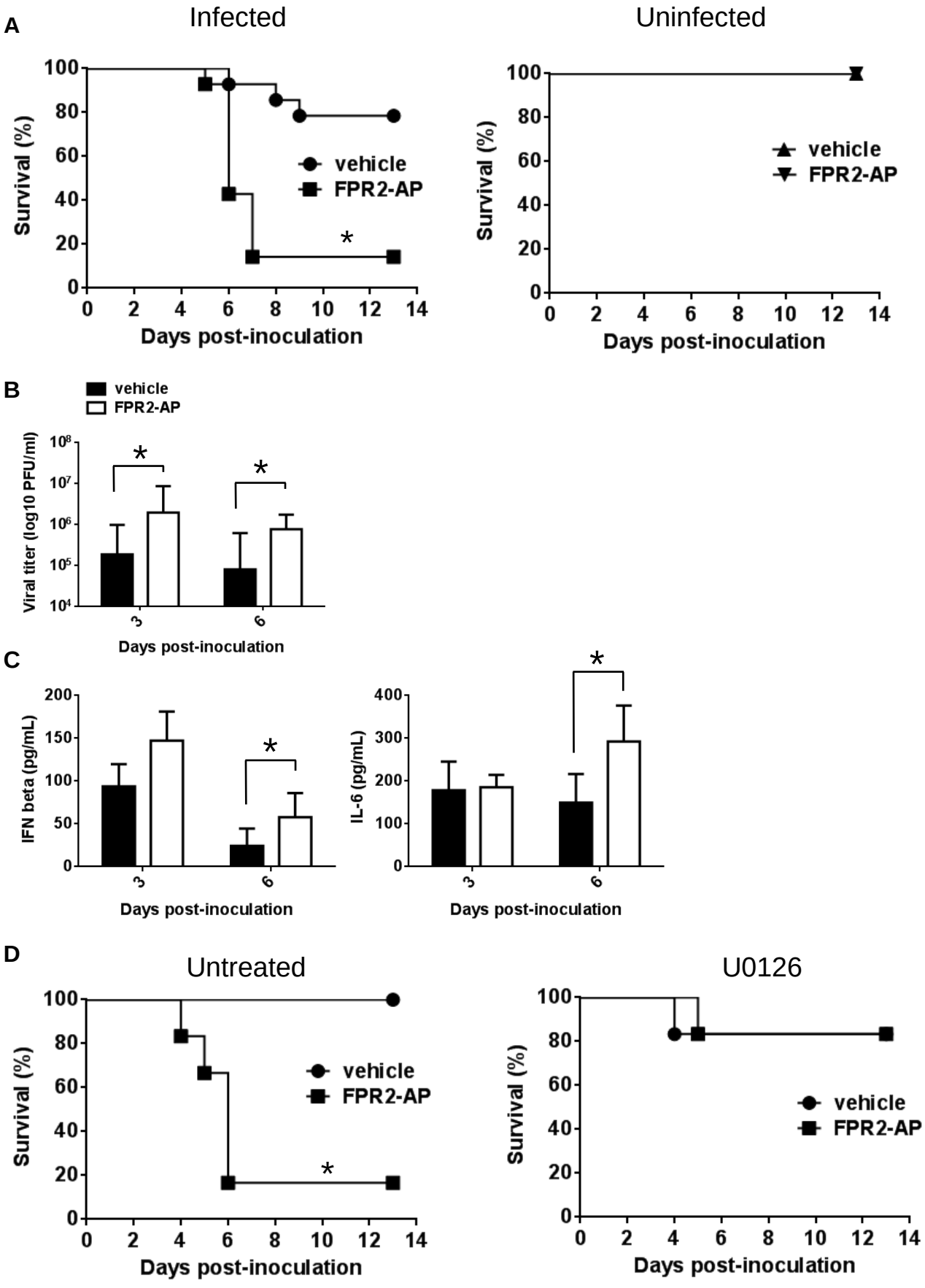
A
Infected
Uninfected
Survival (%)
Days post-inoculation
vehicle
FPR2-AP
*
B
vehicle
FPR2-AP
Viral titer (log10 PFU/ml)
Days post-inoculation
C
IFN beta (pg/mL)
IL-6 (pg/mL)
Days post-inoculation
D
Untreated
U0126
Survival (%)
Days post-inoculation
vehicle
FPR2-AP

Fig 7

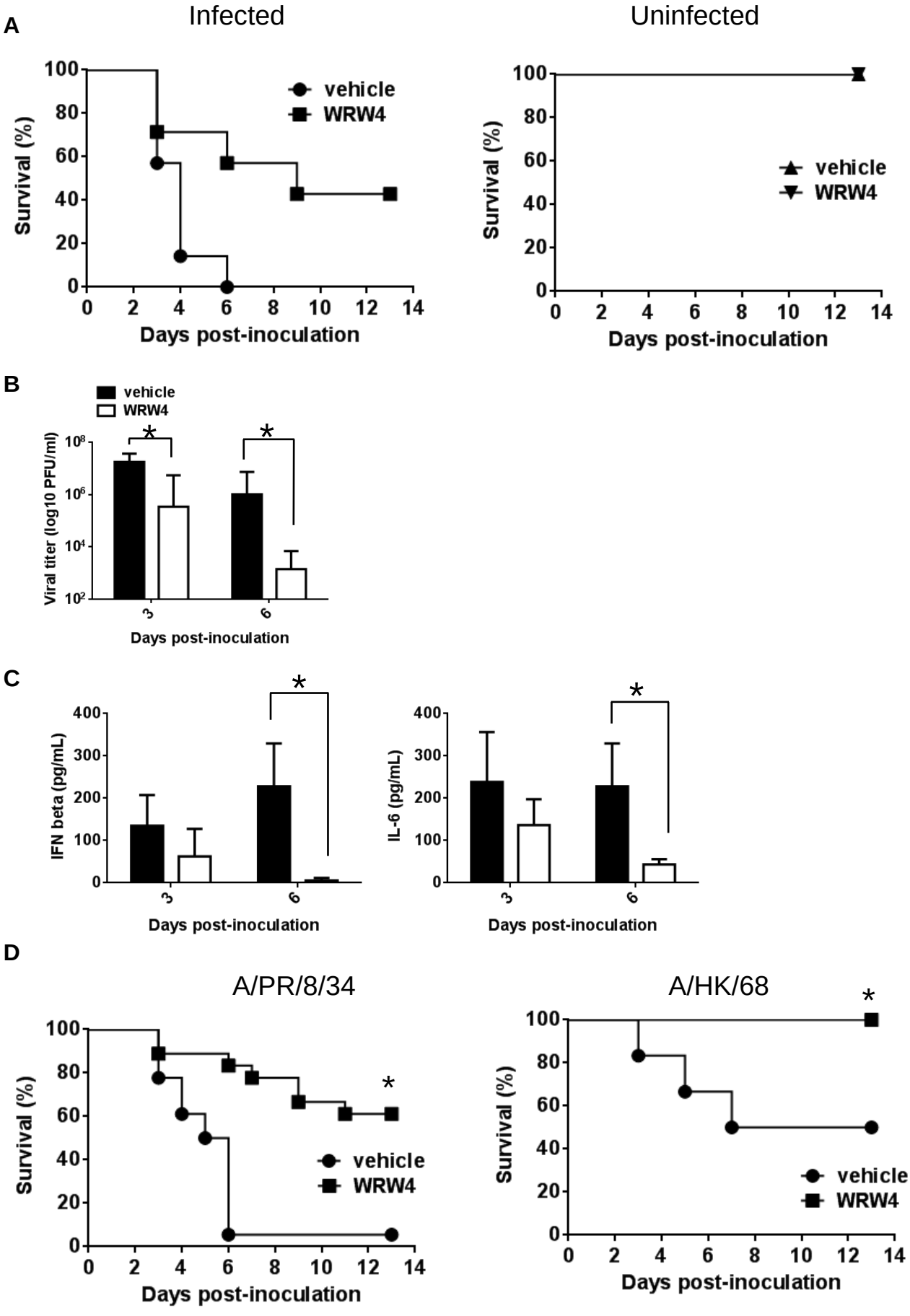
A
Infected
Uninfected
Survival (%)
Days post-inoculation
vehicle
WRW4
B
Viral titer (log10 PFU/ml)
Days post-inoculation
C
IFN beta (pg/mL)
IL-6 (pg/mL)
Days post-inoculation
D
A/PR/8/34
A/HK/68
Survival (%)
Days post-inoculation
vehicle
WRW4